RESEARCH   **Open Access**

Mechanical Performances of Concrete Produced with Desert Sand After Elevated Temperature

Haifeng Liu[1,2]* , Xiaolong Chen[1], Jialing Che[1]*, Ning Liu[1,3] and Minghu Zhang[1]

Abstract

Currently, fire in building is one of the most serious disasters. With the increase of basic construction items in western China, ordinary medium sand resource no longer met with the need of engineering. Compressive strength experiments of concrete produced with desert sand after elevated temperature were carried out in this paper. The effects of desert sand replacement rate (DSRR), temperature and cooling regime on the mechanical performances of concrete produced with desert sand were analyzed. XRD and SEM experiments were also conducted to study the microstructure of concrete produced with desert sand after elevated temperature. Experimental results showed that the cubic compressive strength of concrete produced with desert sand increased firstly, and then declined with temperature. Whereas, the prismatic compressive strength and elasticity modulus of concrete produced with desert sand under static compression declined with temperature. With the enhancement of DSRR, the elasticity modulus under static compression, cubic compressive strength and prismatic compressive strength of concrete produced with desert sand after elevated temperature increased firstly, and then declined, the maximum value of which was reached when DSRR amounted to 40%. Regression models were established to predict the mechanical performances of concrete produced with desert sand after elevated temperature, which were in good agreement with experimental results.

Keywords: concrete, desert sand, prismatic compressive strength, cubic compressive strength, elasticity modulus under static compression, elevated temperature, regression model

1 Introduction

Currently, fire in building occurs frequently and becomes one of the most serious disasters (Li 2005; Guo and Shi 2003). Concrete is used widely in construction industry. When these concrete structures are subjected to building fire or elevated environment, the mechanical performances of which will be weaken. It is imperative to study the mechanical performances of concrete after elevated temperature. The mechanical performance experiments of fiber-reinforced concrete after elevated temperature were carried out by Varona et al. (2018). The compressive strength of ordinary and high- performance concrete declined with temperature, and the strength reduction of ordinary concrete was higher than that of high-performance concrete (Husem 2006). The residual compressive strength of reactive powder concrete increased with temperature when the temperature was below 400 °C and later there was sudden decline in strength (Hiremath and Yaragal 2018; Canbaz 2014; Zheng et al. 2012).

The influences of cooling regime on the properties of concrete were focused by many researchers in recent years. Li et al. (2017) investigated the relation between cement dosage, cooling regime and the recovery of fire-damaged concrete. Husem (2006) studied the mechanical performances of concrete after elevated temperatures under two cooling regimes. The relation

*Correspondence: liuhaifeng1557@163.com; che_jialing@nxu.edu.cn
[1] College of Civil and Hydraulic Engineering, Ningxia University, Yinchuan 750021, China
Full list of author information is available at the end of the article

Liu *et al. Int J Concr Struct Mater*   (2020) 14:26

Page 2 of 15

between different durations, elevated temperatures and the mechanical behaviors of concrete was also researched by Sakr and El-Hakim (2005).

Many researchers had paid numerous attentions on the mechanical performances of concrete produced with solid wastes or industrial by-products after elevated temperature (Ali and Hasan 2008, He and Song 2008, Harun and Ahmet 2008, Isa et al. 2011, Ivanka et al. 2011, Kim et al. 2009, Zhai et al. 2014). With the increase of infrastructure projects in China, more engineering sand was needed. However, there is short of medium sand suitable for engineering in western China. There is abundant desert sand resource in these areas, which belonged to ultra-fine sand. The current national specifications stipulated that the desert sand can't be used as a fine aggregate of concrete (Zhang et al. 2006). To protect natural environment and reduce engineering cost, it's crucial to study the engineering performance of concrete produced with desert sand in China.

Desert sand had been used in many engineering construction in China (Gao et al. 2013, Wang et al. 2011). On the basis of current researches (Padmakumar et al. 2012, Zhenghu et al. 2007), the chemical constituents and particle distribution of desert sand were different greatly from those of ordinary fine sand, medium sand and coarse sand. Because the fineness modulus and particle size of desert sand were smaller than those of other sands, concrete produced with desert sand has the ability of lower strength, poor cohesiveness, bad work performance and low slump.

In order to solve these problems, many researchers had focused on the properties of concrete produced with desert sand. The physical, chemical and other properties of aeolian sand from Indian desert were studied by Padmakumar et al. (2012). The mechanical properties of concrete produced with dune sand were also researched (Al-Harthy et al. 2007, Chaabane et al. 2017 and Al-Sanad et al. 1993). Jin et al. (2012) carried out experiments to study the mechanical performances of concrete and mortar produced with Tenggeli and Mu Us desert sand. Chuah et al. (2016) performed the mechanical properties, microanalysis, porosity, sorptivity and air void experiment of geopolymer mortars produced with dune sand. Split Hopkinson pressure bar (SHPB) was used to carry out dynamic compression experiment to study the influence of impact speed and DSRR on the dynamic behaviors of concrete produced with desert sand (Liu et al. 2016, 2017b).

In this paper, desert sand from Mu Us sandy land in Yanchi country was used as fine aggregate. The effects of DSRR, temperature and cooling regime on the elasticity modulus under static compression, cubic compressive strength and prismatic compressive strength of concrete

produced with desert sand were analyzed. The influence of temperature on the microstructure of concrete produced with desert sand was also analyzed according to XRD and SEM.

2 Experimental Investigations
2.1 Material
42.5R Portland cement branded as Saima was employed for all concrete mixtures, the original and final set time of which were 135 min and 174 min. Compressive strength at 3 days and 28 days were 33.4 and 54.8 MPa.

Coarse aggregate was two-grade crushed stone. The size of big stone ranged from 10 to 20 mm and size of small stone was from 5 to 10 mm. The weight ratio of big stone to small stone was 7:3. Apparent density, packing density, void fraction and mud content of coarse aggregate were 2698 kg/m^3, 1430 kg/m^3, 47% and 0.78%.

Fine aggregate comprised local medium sand and desert sand. Apparent density, packing density and void fraction of local medium sand were 2636 kg/m^3, 1570 kg/m^3 and 41.9%, the mud content and fineness modulus of which were 0.6% and 2.38. Desert sand was obtained from Mu Us sandy land in Yanchi country, Ningxia, the apparent density, packing density and void fraction of which were 2624 kg/m^3, 1400 kg/m^3 and 40.95%. Mud content and fineness modulus were only 0.14% and 0.292. The chemical compositions of medium sand and desert sand used in this paper were given in previous studies (Liu et al. 2016, 2017a, 2017b). Figure 1 showed the particle distribution of local medium sand and desert sand. Primary fly ash was provided by local power plant, the fineness (45 μm sieve residue), water content, SO$_3$ content and loss on ignition of which were 9.2%, 0.2%, 0.2% and 2.8%. To improve the performance of concrete,
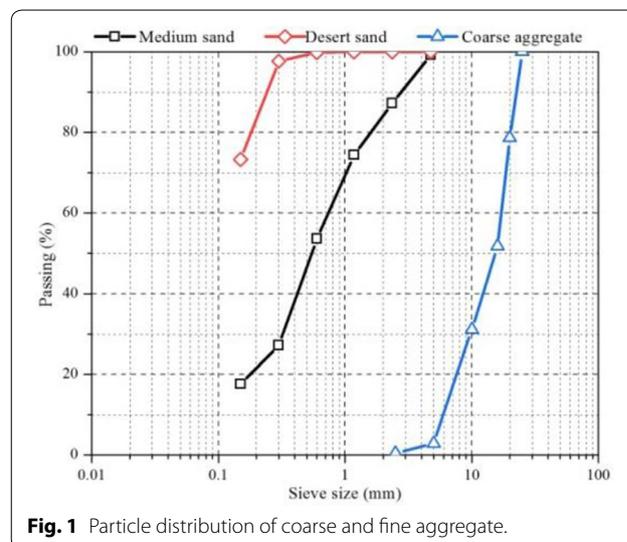
Fig. 1 Particle distribution of coarse and fine aggregate.

Liu *et al. Int J Concr Struct Mater*   (2020) 14:26

Page 3 of 15

polycarboxylic super-plasticizer produced by Beijing Muhu Company was used, the water reduction and solid content of which were above 25% and 98%. For mixing and curing concrete specimens, local potable water was employed.

2.2 Specimen Fabrication
Concrete specimens with different DSRR and fly ash replacement ratios were made. DSRR varied from 0 to 100% with the increment of 20% while fly ash replacement ratio was 0% and 10%. Water binder ratio, sand ratio and dosage of water were 0.45, 0.32 and 190 kg/m³. Specific mix ratio of concrete produced with desert sand was listed in Table 1. Dosage of super-plasticizer was 0.3% that of cementing material. Cubic specimens with the dimension of 100 mm × 100 mm × 100 mm were made to test cubic compressive strength while prismatic specimens with the dimension of 100 mm × 100 mm × 300 mm were prepared to test elasticity modulus under static compression and prismatic compressive strength of concrete produced with desert sand.

According to Chinese Standard (GB/T 50081-2002) (2002), raw materials were strictly weighed. Firstly, coarse aggregate was added into forced agitator working 30 s, followed by cement, fly ash and fine aggregate. Then, super-plasticizer was sufficiently mixed with water and put into agitator working 60 s. After finishing the process of stir, compound concrete was put into plastic moulds and vibrated on shaking table until the appearance of cement paste on the surface of specimens. Specimens were demolded after keeping 24 h at room temperature and removed to standard curing room for 28 days curing.

2.3 Experiment Design
After 28 days curing, the specimens were moved out of standard curing room. To avoid the burst of specimens, the specimens were dried in an oven for 4 h with the temperature of 80 ℃. Then, CSL-26-17 heating furnace with a ultimate temperature of 1600 ℃ was used to carry out elevated temperature test. Target temperatures were 100 ℃, 300 ℃, 500 ℃ and 700 ℃. The temperature-rising curve was shown in Fig. 2.

After removal from heating furnace, the specimens were conducted by two cooling regimes: natural cooling at room temperature or water cooling for 0.5 h. After cooling finished, all specimens were stood in laboratory at room temperature for 4 days, dried and weighed again. Then, the specimens were used to carry out compressive strength experiments of concrete produced with desert sand.

3 Analysis of Experimental Results
3.1 Cubic Compressive Strength
Figure 3 showed typical pictures of concrete specimen T5 after different temperatures. Under the condition of natural cooling, the appearance of specimen T5 after 100 ℃ was dark grey, which was similar to that at room temperature. The appearance of specimen T5 after 300 ℃ became darker with local yellowing, and then became faint yellow after 500 ℃. Some micro-cracks were nucleated and stretched from edge to the middle part of specimen. The appearance of specimen T5 after 700 ℃ was offwhite with yellow spot and had a burst
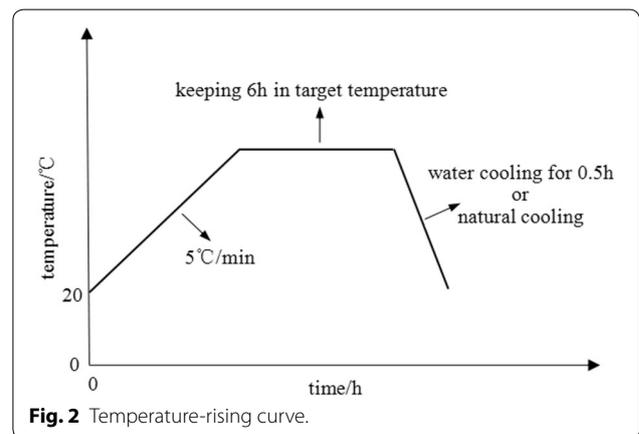
Fig. 2 Temperature-rising curve.

Table 1 Specific mix ratio of concrete produced with desert sand.

No	Fly ash replacement ratio/%	DSRR/%	Quality of material/kg m⁻³						
			Water	Cement	Fly ash	Medium sand	Desert sand	Big stone	Small stone
T0	0	0	190	422	0	572	0	851	365
T1	10	0	190	380	46	572	0	851	365
T2		20	190	380	46	458	114	851	365
T3		40	190	380	46	343	229	851	365
T4		60	190	380	46	229	343	851	365
T5		80	190	380	46	114	458	851	365
T6		100	190	380	46	0	572	851	365

Liu *et al. Int J Concr Struct Mater*   (2020) 14:26

Page 4 of 15

Fig. 3 Pictures of specimen T5 after different temperatures.
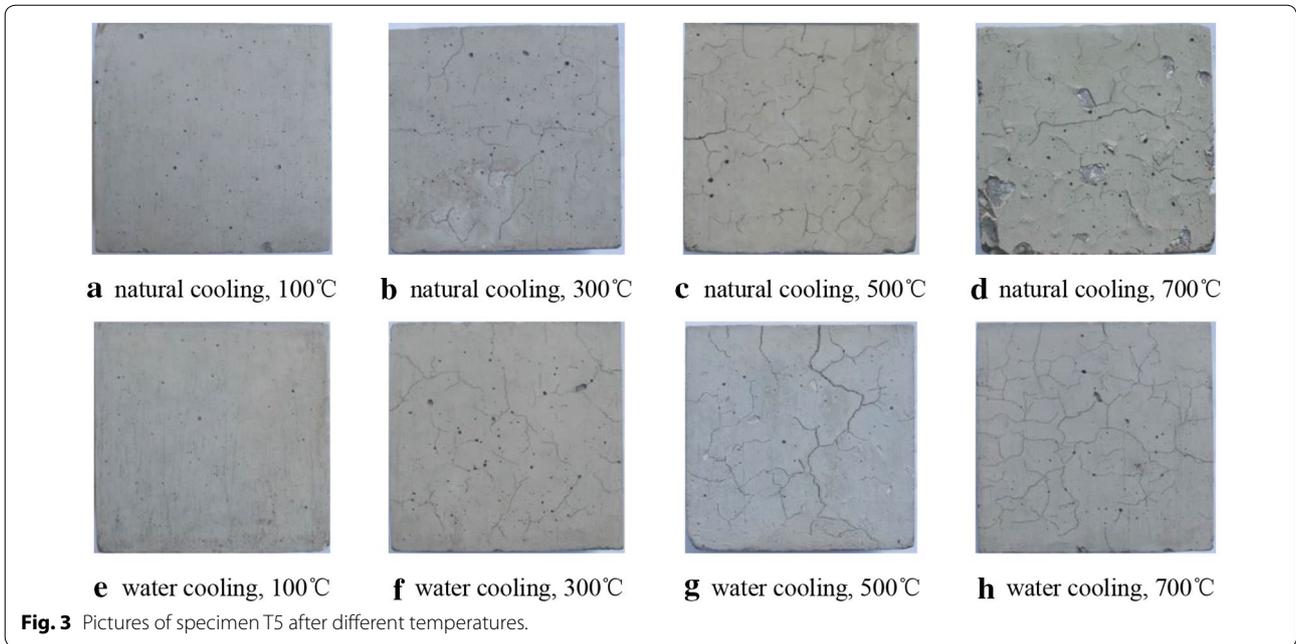
of spalling. Compared with specimen T5 after 500 °C, there were more uniformly distributed micro-cracks on the surface of specimen T5 after 700 °C. Under the condition of water cooling, the appearance of specimens T5 after 100 °C, 300 °C, 500 °C and 700 °C was gray, buff, light yellow and French grey with short capillary crack.

Experimental results of cubic compressive strength of concrete produced with desert sand after elevated temperature were listed in Table 2. Figure 4 showed the relation between cubic compressive strength of concrete produced with desert sand and temperature. It can be seem from Fig. 4 and Table 2 that the cubic compressive strength of concrete produced with desert sand increased firstly, and then declined with temperature, the

maximum value of which was reached with the temperature of 100 °C.

Relation between the cubic compressive strength of concrete produced with desert sand and DSRR was shown in Fig. 5. Figure 5 showed that the cubic compressive strength of concrete produced with desert sand increased firstly, and then declined with DSRR. When DSRR amounted to 40%, the cubic compressive strength of concrete produced with desert sand arrived at the maximum value, which can be explained in the following way. Particle size of desert sand was so small that desert sand filled with gaps between coarse aggregate and medium sand, which made concrete more uniformly. At the same time, desert sand came from the long-term weathering formation of loose parent rock, the strength of which was lower than that of ordinary

Table 2 Cubic compressive strength of concrete produced with desert sand after elevated temperature.

Cooling regime	Temperature	Cubic compressive strength/MPa					
		T1	T2	T3	T4	T5	T6
Natural cooling	Room temperature	47.67	48.79	51.09	48.29	46.85	43.67
	100 °C	50.82	51.62	56.24	53.54	48.57	47.07
	300 °C	48.50	50.77	56.31	54.94	51.02	47.37
	500 °C	42.26	47.58	49.65	44.38	42.05	40.79
	700 °C	34.06	34.55	35.20	31.50	30.84	30.00
Water cooling	Room temperature	47.67	48.79	51.09	48.29	46.85	43.67
	100 °C	48.89	49.71	51.87	51.11	47.93	44.56
	300 °C	43.68	44.39	48.35	47.59	45.55	41.47
	500 °C	40.22	40.85	41.77	41.33	39.37	37.92
	700 °C	30.32	30.64	30.47	30.30	30.00	29.71

Liu *et al. Int J Concr Struct Mater* (2020) 14:26

Page 5 of 15

Fig. 4 Relation between the cubic compressive strength of concrete produced with desert sand and temperature.

Fig. 5 Relation between the cubic compressive strength of concrete produced with desert sand and DSRR.
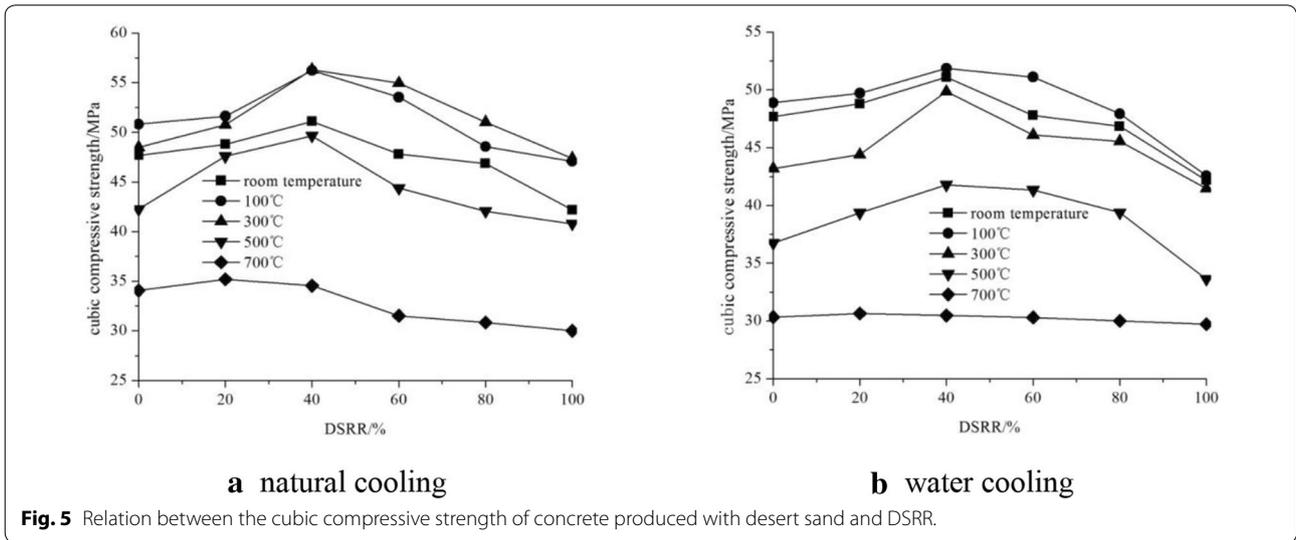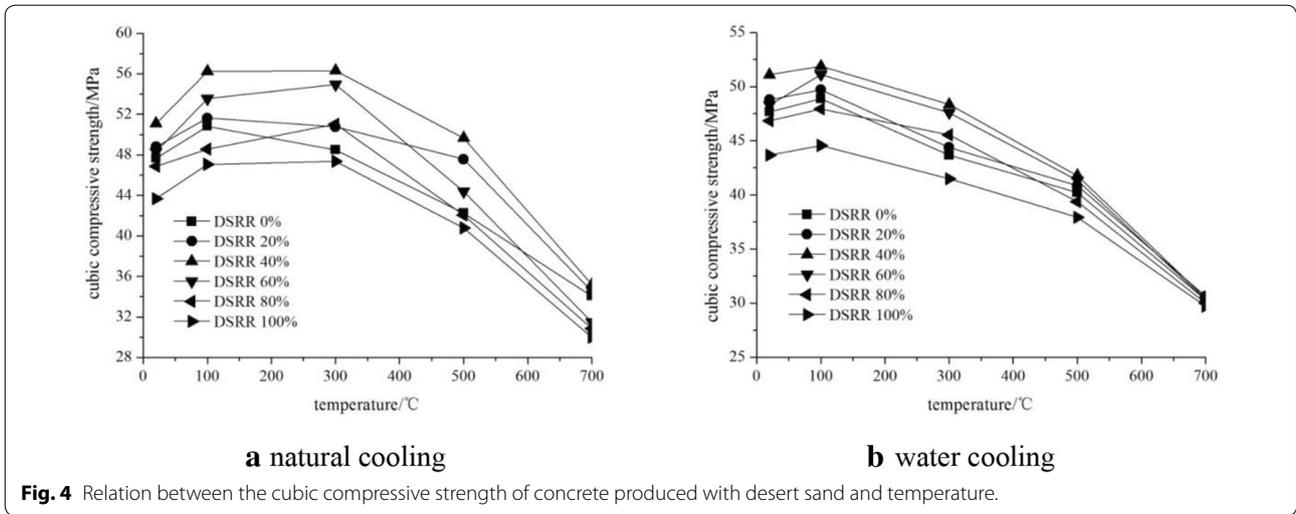
medium sand. So, with the enhancement of DSRR, the cubic compressive strength of concrete produced with desert sand increased firstly, and then declined.

To assess cubic compressive strength of concrete produced with desert sand after elevated temperature, a regression model among cubic compressive strength $f_c(t,s)$, temperature t and DSRR s was established. Comparison between the experimental results and predicted results from the model was shown in Fig. 6. Figure 6 showed that the predicted results were in good agreement with the experimental results.

Under the condition of natural cooling,

$$\frac{f_c(t,s)}{f_c} = 1.01131 + 0.00424s + 0.49251\left(\frac{t-20}{700}\right) - 0.86187\left(\frac{t-20}{700}\right)^2 \tag{1}$$

where f_c was the cubic compressive strength of ordinary concrete T0 at room temperature, MPa; t was temperature, °C; s was DSRR, %.

Determination coefficient R^2 and COV value of above model were 0.9532 and 0.0328, which showed that model fitting degree was good. Test probability of the model was equal to 0.0001, which was far less than 0.05. So the model was effective to predict the cubic compressive strength of concrete produced with desert

Liu *et al. Int J Concr Struct Mater* (2020) 14:26

Page 6 of 15

Fig. 6 Comparison of cubic compressive strength between the predicated results from the regression model and experimental results of concrete produced with desert sand.
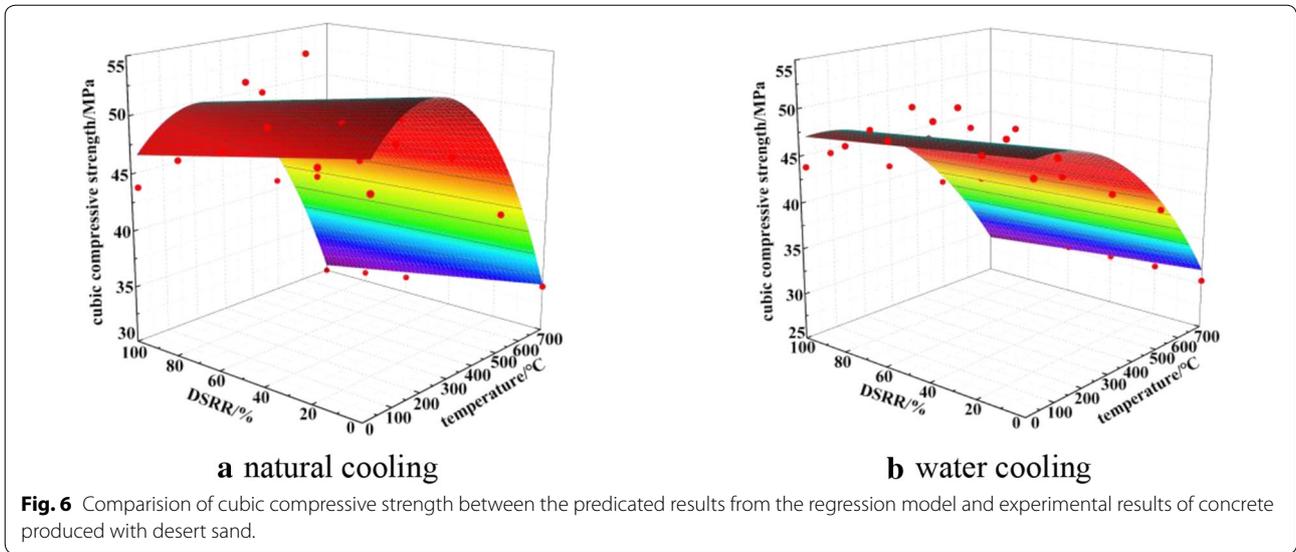
sand after elevated temperature under the condition of natural cooling.

Under the condition of water cooling,

$$\frac{f_c(t,s)}{f_c} = 0.99634 + 0.02522s + 0.06267\left(\frac{t-20}{700}\right)$$
$$- 0.45916\left(\frac{t-20}{700}\right)^2 \quad (2)$$

Determination coefficient R^2 and COV value of above model were 0.9701 and 0.0243, which indicated the model was effective to predict the cubic compressive strength of concrete after elevated temperature under the condition of water cooling.

Figure 7 showed relation between the cubic compressive strength of T3 and temperature under different cooling regimes. The cubic compressive strength of T3 under the condition of natural cooling was larger than that under the condition of water cooling. This can be explained in the following way. Different from natural cooling, concrete specimen produced with desert sand under the condition of water cooling was cooled by water suddenly. Violent expansion due to heat and contraction produced stress difference, which finally led to strength reduction.

3.2 Prismatic Compressive Strength

Mass loss rate was the ratio of mass difference before and after elevated temperature to specimen mass before elevated temperature, which was listed in Table 3. Figure 8 showed relation between the mass loss rate of concrete produced with desert sand and temperature. The mass

Fig. 7 Relation between cubic compressive strength of T3 and temperature under different regimes.
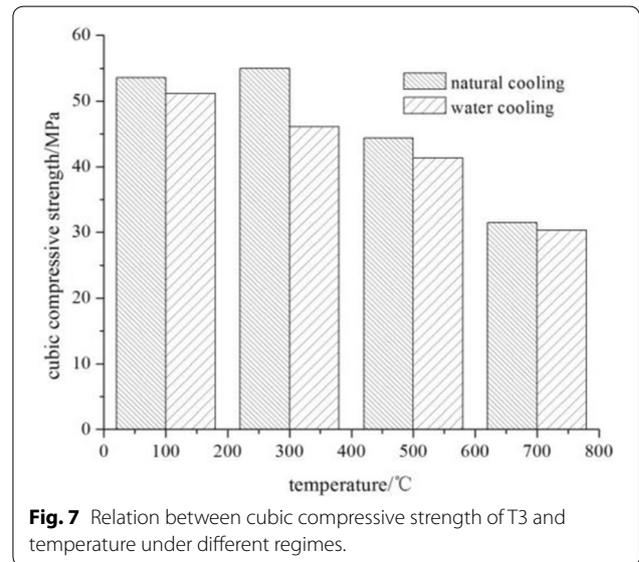
loss rate of concrete produced with desert sand increased with temperature, which enhanced more quickly when the temperature was below 300 °C than that above 300 °C. This can be explained in the following way. Free water and adsorption water in specimen evaporated with temperature. When the temperature amounted to 300 °C, the volume evaporation of free water and adsorption water reached the maximum value, and then declined with temperature. At the same time, chemical bonding water in hardened cement mortar began to decompose, which made the mass loss rate of concrete produced with desert sand increase with temperature (Sun and Miu 2012).

Liu *et al. Int J Concr Struct Mater* (2020) 14:26

Page 7 of 15

Table 3 Mass loss rate of concrete produced with desert sand after elevated temperature.

Cooling regime	Temperature	Mass loss rate/%				
		T1	T2	T3	T4	T5
Natural cooling	Room temperature	0	0	0	0	0
	100 °C	1.88	1.78	1.76	1.75	1.73
	300 °C	5.18	5.48	5.78	5.45	6.78
	500 °C	5.93	5.88	6.37	5.86	6.80
Water cooling	Room temperature	0	0	0	0	0
	100 °C	1.37	1.29	1.57	0.96	1.65
	300 °C	3.71	4.12	4.26	3.49	2.51
	500 °C	4.84	4.96	4.44	4.86	4.74

a natural cooling **b** water cooling
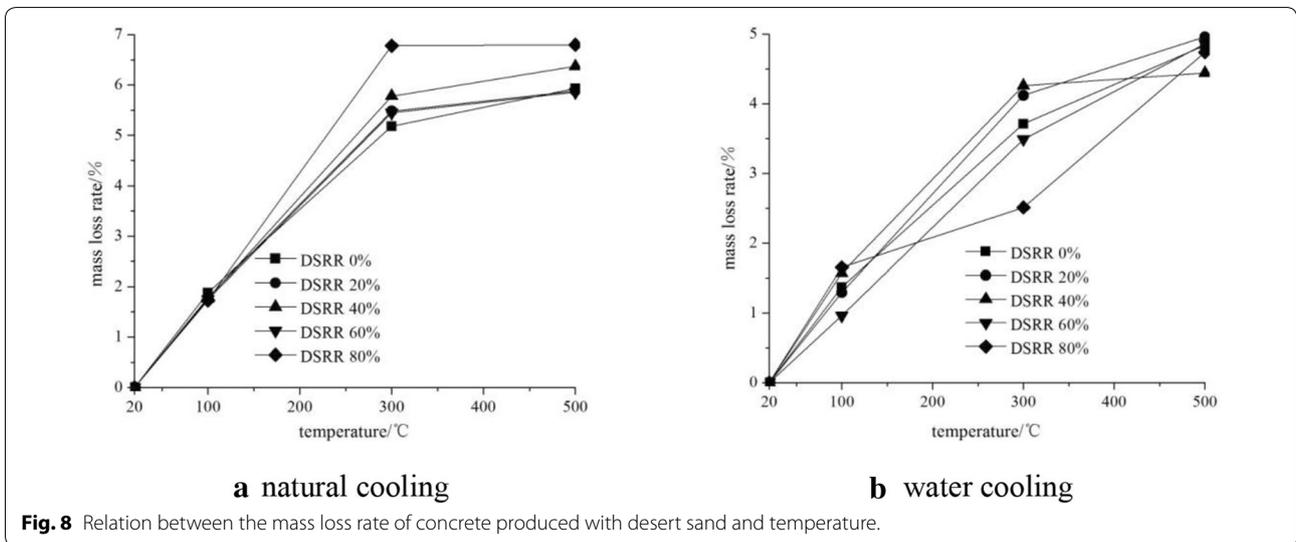
Fig. 8 Relation between the mass loss rate of concrete produced with desert sand and temperature.
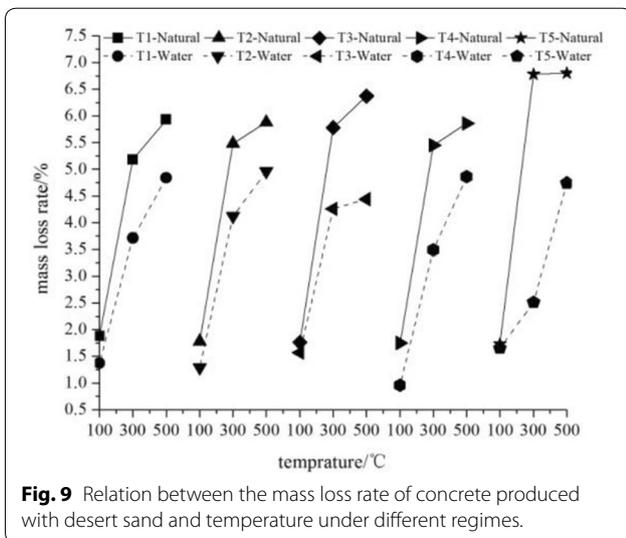
Fig. 9 Relation between the mass loss rate of concrete produced with desert sand and temperature under different regimes.

Relation between the mass loss rate of concrete produced with desert sand and temperature under different regimes was shown in Fig. 9. The mass loss rate of concrete produced with desert sand after elevated temperature under the condition of water cooling were less than that under the condition of natural cooling.

The experimental results of prismatic compressive strength of concrete produced with desert sand after elevated temperature were listed in Table 4. Figure 10 showed relation between the prismatic compressive strength of concrete produced with desert sand and temperature. The prismatic compressive strength of concrete produced with desert sand declined with temperature.

Relation between prismatic compressive strength of concrete produced with desert sand after elevated temperature and DSRR was showed in Fig. 11. Figure 11 showed that the prismatic compressive strength of

Liu *et al. Int J Concr Struct Mater*   (2020) 14:26

Page 8 of 15

Table 4 Prismatic compressive strength of concrete produced with desert sand after elevated temperature.

Cooling regime	Temperature	Prismatic compressive strength/MPa				
		T1	T2	T3	T4	T5
Natural cooling	Room temperature	31.70	31.93	35.00	32.55	32.10
	100 °C	30.35	30.55	32.32	31.97	30.05
	300 °C	18.92	20.75	23.44	21.14	22.47
	500 °C	9.80	10.98	12.42	11.66	12.10
Water cooling	Room temperature	31.70	31.93	35.00	32.55	32.10
	100 °C	30.31	30.47	31.95	31.32	29.22
	300 °C	16.80	18.78	21.21	16.85	16.53
	500 °C	9.57	10.84	11.95	11.52	11.68
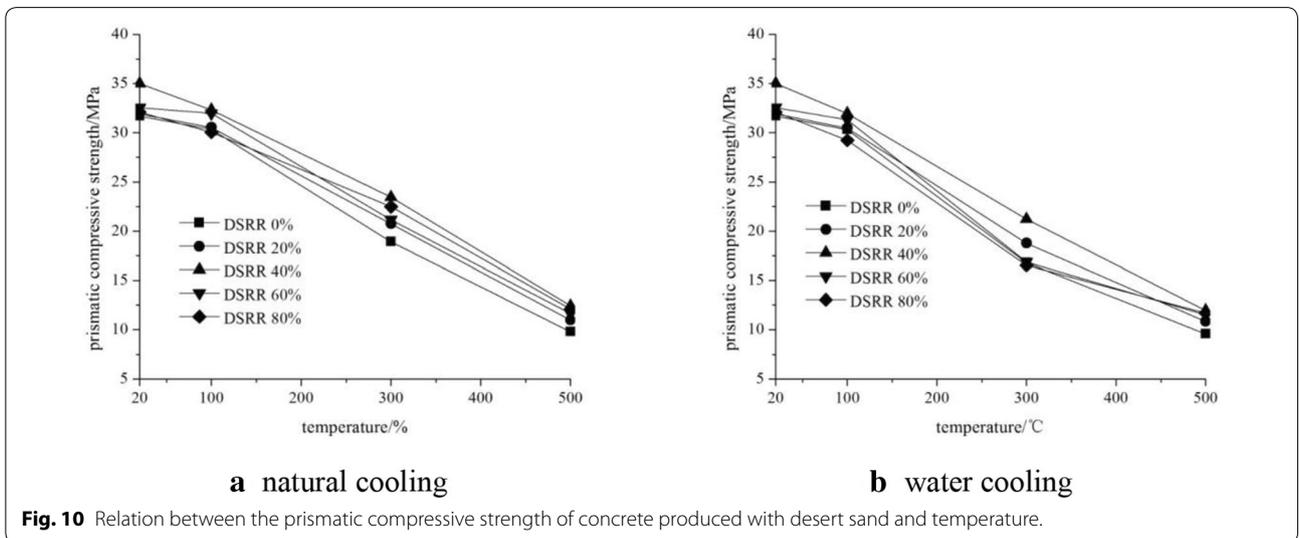
a natural cooling   **b** water cooling

Fig. 10 Relation between the prismatic compressive strength of concrete produced with desert sand and temperature.

a natural cooling   **b** water cooling

Fig. 11 Relation between the prismatic compressive strength of concrete produced with desert sand and DSRR.

Liu *et al. Int J Concr Struct Mater*   (2020) 14:26

Page 9 of 15
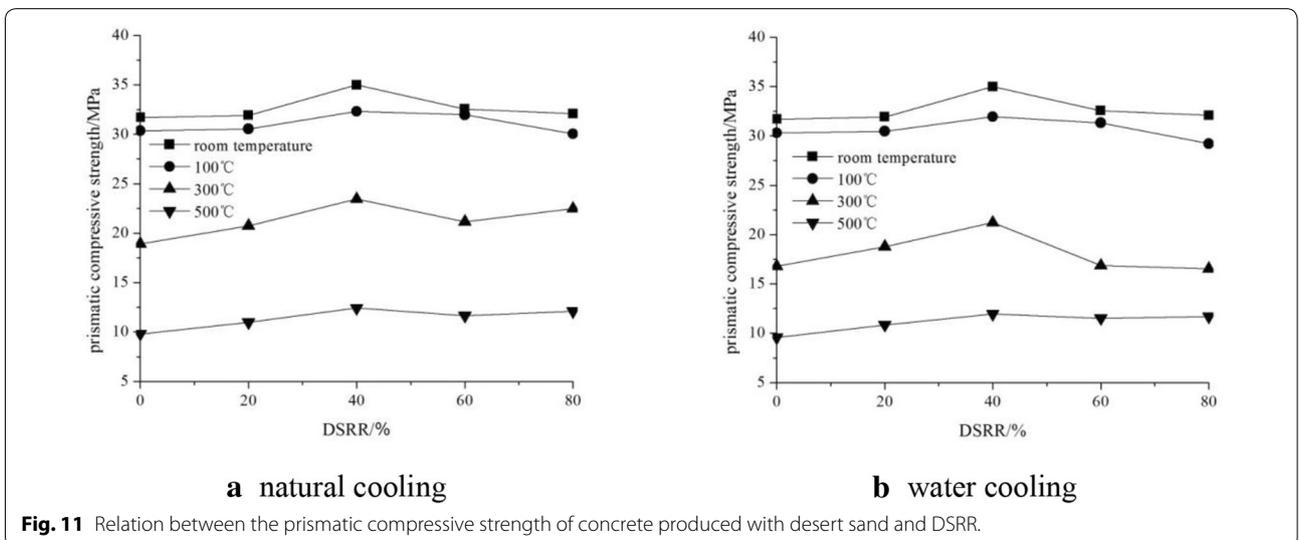
concrete produced with desert sand after elevated temperature increased firstly, and then declined with DSRR, the maximum value of which was obtained when DSRR amounted to 40%.

Based on the analysis of experimental results, a regression model among prismatic compressive strength, temperature and DSRR was established. Comparison between the experimental results and predicated results from the model was shown in Fig. 12. It can be seem from Fig. 12 that the predicted results agreed well with the experimental results.

Under the condition of natural cooling,

$$\frac{f_c'(t,s)}{f_c'} = 0.99728 + 0.04237s - 0.71728\left(\frac{t-20}{700}\right) - 0.378\left(\frac{t-20}{700}\right)^2 \tag{3}$$

where f_c' was the prismatic compressive strength of ordinary concrete T0 at room temperature, MPa.

Determination coefficient R^2 and COV value of above model were 0.9752 and 0.0356. So the model was effective to predict the prismatic compressive strength of concrete produced with desert sand after elevated temperature under the condition of natural cooling.

Under the condition of water cooling,

$$\frac{f_c'(t,s)}{f_c'} = 1.0321 - 0.00575s - 1.27391\left(\frac{t-20}{700}\right) + 0.37327\left(\frac{t-20}{700}\right)^2 \tag{4}$$

Fig. 13 Relation between the prismatic compressive strength of concrete produced with desert sand and temperature under different regimes.
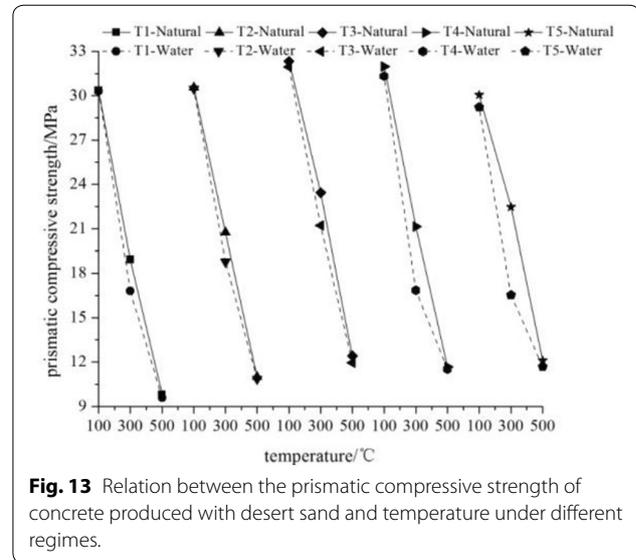
Determination coefficient R^2 and COV value of above model were 0.9756 and 0.0614, which indicated that the model was effective to predict the prismatic compressive strength of concrete produced with desert sand under the condition of water cooling.

Figure 13 showed relation between prismatic compressive strength of concrete produced with desert sand and temperature under different cooling regimes. As shown in Fig. 13, the prismatic compressive strength of concrete produced with desert sand under the condition of water cooling was less than that under the condition of natural cooling.

a natural cooling   **b** water cooling

Fig. 12 Comparison of prismatic compressive strength between the predicated results from the regression model and experimental results of concrete produced with desert sand.

Liu *et al. Int J Concr Struct Mater*   (2020) 14:26

Page 10 of 15
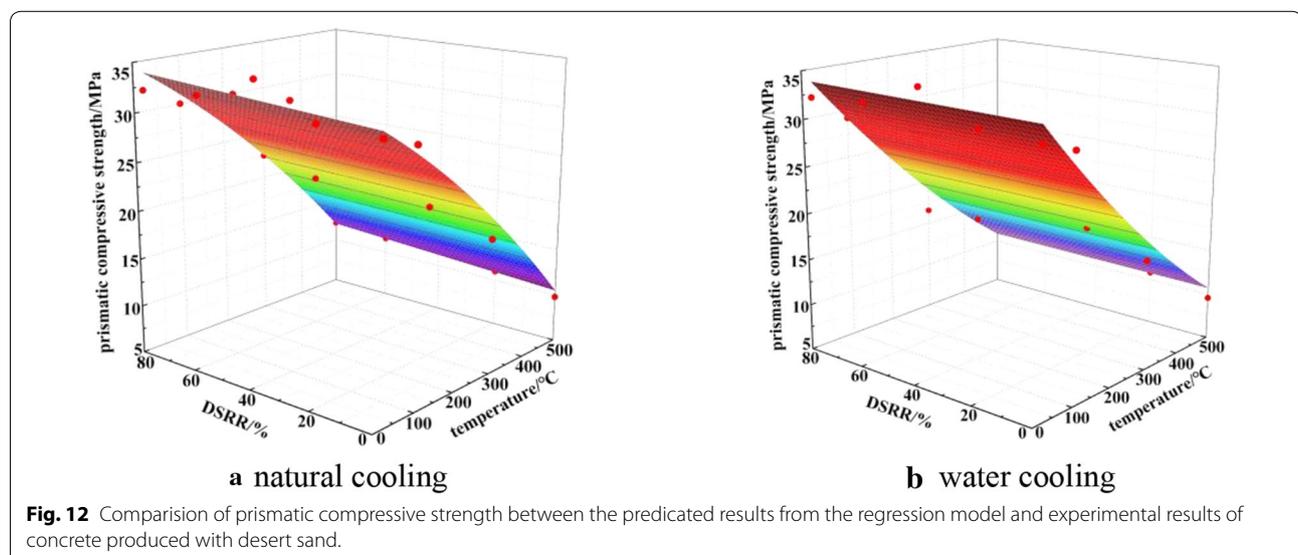
3.3 Elasticity Modulus Under Static Compression

Elasticity modulus of concrete under static compression after elevated temperature was calculated in accordance with Chinese Standard (GB/T 50081-2002),

$$E = \frac{(F_a - F_0)}{A} \cdot \frac{L}{\Delta N} \qquad (5)$$

where F_0 was load when stress in the cross section of specimen reached 0.5 MPa; A was the cross section area of specimen; F_a was load when stress in the cross section of specimen reached one-third prismatic compressive strength of concrete; L was gauge length; ΔN was displacement difference measured by dial gages on both sides of specimen under the action of load F_a and F_0 (GB/T 50081-2002).

The experimental results of elasticity modulus of concrete produced with desert sand after elevated temperature were listed in Table 5. Figure 14 showed relation between the elasticity modulus of concrete produced with desert sand and temperature. As shown in Fig. 14 and Table 5, the elasticity modulus of concrete produced with desert sand declined with temperature.

Relation between the elasticity modulus of concrete produced with desert sand and DSRR was showed in Fig. 15. The elasticity modulus of concrete produced with desert sand after elevated temperature increased firstly, and then declined with DSRR. The elasticity modulus of concrete produced with desert sand after elevated temperature reached the maximum value when DSRR amounted to 40%.

On the basis of experimental results, a regression model among elasticity modulus under static compression, temperature and DSRR was established. Figure 16 showed the comparison between the experimental results and predicated results from the model, which indicated that the predicted results agreed well with the experimental results.

Under the condition of natural cooling,

Table 5 Elasticity modulus of concrete produced with desert sand after elevated temperature.

Cooling regime	Temperature	Elasticity modulus of concrete/GPa				
		T1	T2	T3	T4	T5
Natural cooling	Room temperature	34.54	34.59	35.32	31.76	30.73
	100 ℃	31.39	31.73	32.26	31.06	30.50
	300 ℃	10.75	11.39	11.59	9.72	8.21
	500 ℃	3.99	4.41	5.29	4.85	3.65
Water cooling	Room temperature	34.54	34.59	35.32	31.76	30.73
	100 ℃	29.84	29.93	30.24	29.21	30.04
	300 ℃	7.72	9.46	10.01	8.90	7.60
	500 ℃	3.86	3.91	4.48	4.37	3.33

a natural cooling   **b water cooling**
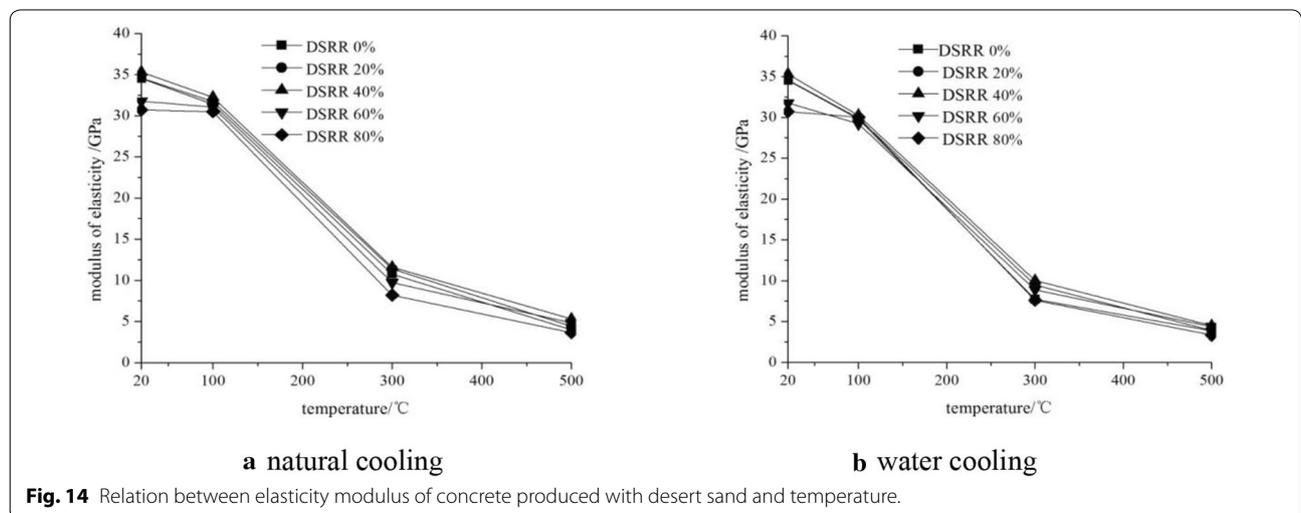
Fig. 14 Relation between elasticity modulus of concrete produced with desert sand and temperature.

Liu *et al. Int J Concr Struct Mater*   (2020) 14:26

Page 11 of 15

Fig. 15 Relation between the elastic modulus of concrete produced with desert sand and DSRR.

Fig. 16 Comparision of elasticity modulus between the predicated results from the regression model and experimental results of concrete produced with desert sand.
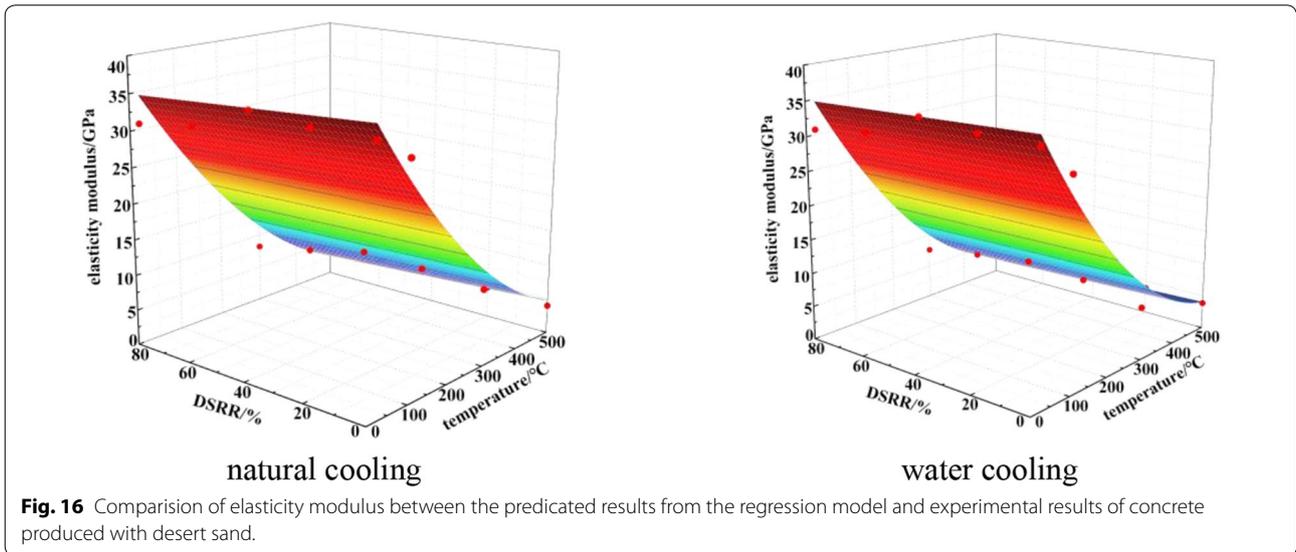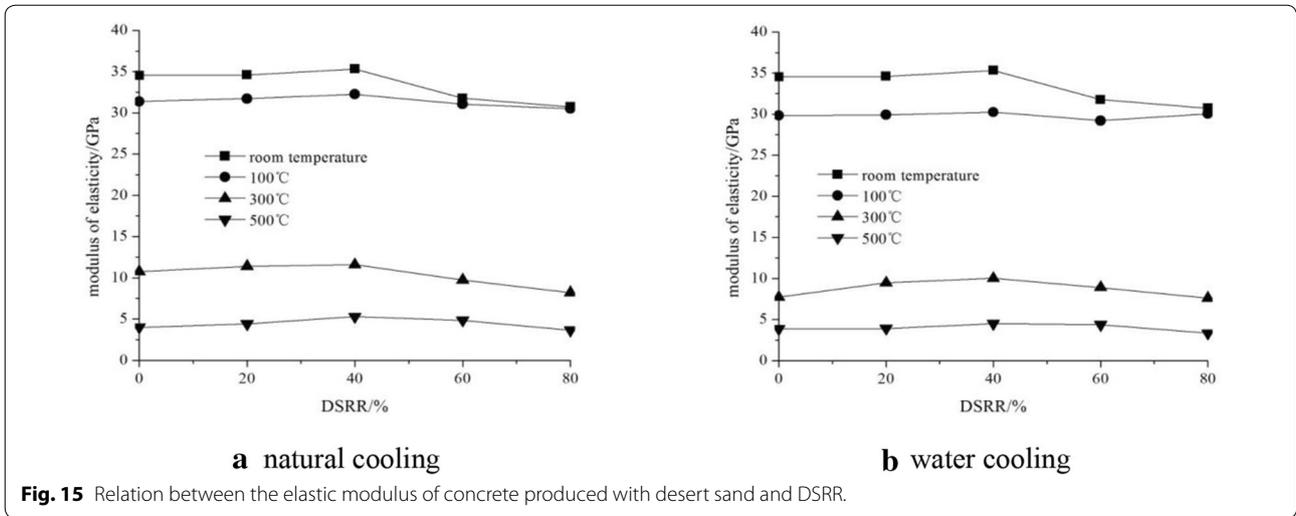
$$\frac{E_c(t,s)}{E_c} = 1.0597 + 0.01855s - 2.22002\left(\frac{t-20}{700}\right)$$
$$+ 1.21061\left(\frac{t-20}{700}\right)^2 \quad (6)$$

where E_c was the elasticity modulus of ordinary concrete T0 at room temperature, GPa.

Determination coefficient R^2 and COV value of above model were 0.9594 and 0.0731, which indicated that the model was effective to predict the elasticity modulus of concrete produced with desert sand after elevated temperature under the condition of natural cooling.

Under the condition of water cooling,

$$\frac{E_c(t,s)}{E_c} = 1.04214 + 0.04422s - 2.49082\left(\frac{t-20}{700}\right)$$
$$+ 1.59704\left(\frac{t-20}{700}\right)^2 \quad (7)$$

Determination coefficient R^2 and COV value of the model was 0.9671 and 0.0748. So the model was effective to predict the elasticity modulus of concrete produced with desert sand after elevated temperature under the condition of water cooling.

Relation between the elasticity modulus of concrete produced with desert sand and temperature under different cooling regimes was shown in Fig. 17. The
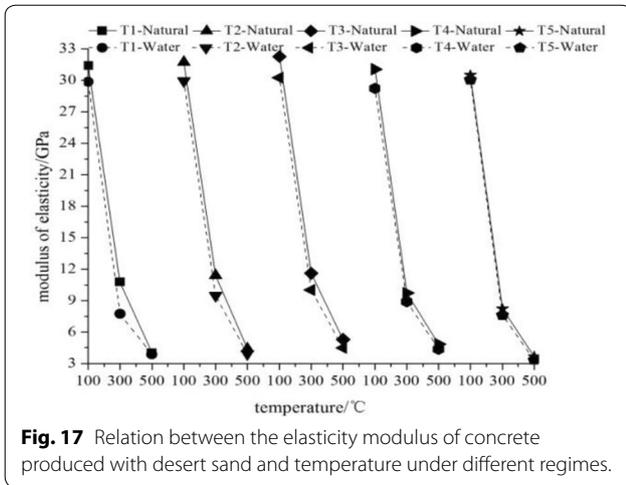
Fig. 17 Relation between the elasticity modulus of concrete produced with desert sand and temperature under different regimes.

Table 6 Elasticity modulus of concrete T0 and T1 after elevated temperature.

Cooling regime	No	Elasticity modulus of concrete/GPa			
		Room temperature	100 °C	300 °C	500 °C
Natural cooling	T0	35.31	30.38	9.53	3.68
	T1	37.46	31.39	10.75	3.99
Water cooling	T0	35.31	29.60	7.13	3.78
	T1	37.46	29.84	7.72	3.86
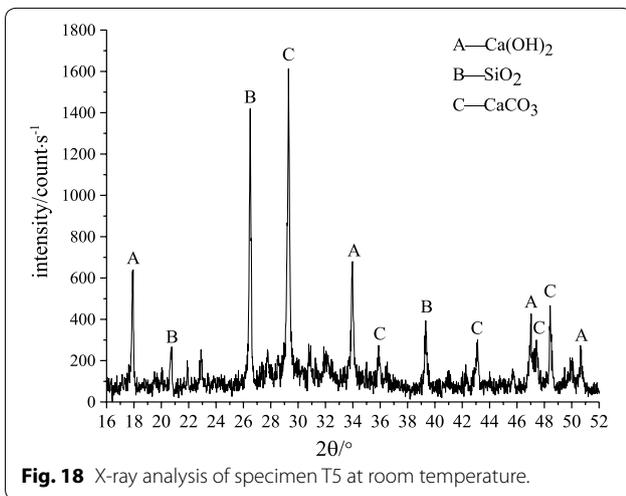
Fig. 18 X-ray analysis of specimen T5 at room temperature.

elasticity modulus of concrete produced with desert sand under the condition of water cooling was less than that under the condition of natural cooling.

The elasticity modulus of concrete T0 and T1 after different temperatures was listed in Table 6. As listed in Table 6, the elasticity modulus of T1 was larger than that of T0.

4 Microstructure of Concrete Produced with Desert Sand After Elevated Temperature

Figure 18 showed X-ray analysis of specimen T5 at room temperature. In addition to original cement clinker and aggregate, new calcium hydroxide (CH) and calcium silicate hydrate(C-S-H) were produced. There is no obvious characteristic peak of Trisulfide hydrated calcium sulphoaluminate (AFt), which can be expressed in following way. AFt crystal began to be decomposed at 80 °C (Sun and Miu 2012). In our experiment, in order to avoid the burst of specimen, all specimens had been dried in an oven for 4 h with the temperature of 80 °C before elevated temperature test. So the characteristic peak of AFt was difficult to be discerned.

X-ray analysis of specimen T5 after different temperatures was showed in Fig. 19. The peak intensity of CH declined with temperature, the maximum value of which was reached at room temperature. Whereas, the peak intensity of $CaCO_3$ increased firstly, and then declined with temperature. When the temperature was equal to 300 °C, the peak intensity of $CaCO_3$ reached the maximum value.

Figure 20 showed SEM of specimen T5 after different temperatures. At room temperature, specimen T5 was inner structurally-complete and had good compactness. C-S-H was dark gray floc while CH was white stacked crystal. Unhydrated spherical gel particles (fly ash or cement particle) were distributed in the section of cement matrix. After 300 °C, flocculent gel structure system of CH became more compact. The interface between coarse aggregate and cement mortar was more distinct. After 500 °C, the intensity of intact layered CH decreased, which may be caused by the lost of water content in cement hydration products and decomposition of C-S-H (Sun and Miu 2012). Many small pores were produced and micro-cracks were nucleated between coarse aggregate and cement mortar. The whole structure was loose. After 700 °C, the intensity of CH reduced further. Cement matrix became more shriveled. Some micro-cracks stretched and interacted with each other. At the same time, more new micro-cracks were nucleated. White large crystals CH were scarce.

5 Conclusions

In this paper, the effect of DSRR, temperature and cooling regime on the mechanical performances of concrete produced with desert sand was analyzed. To study the
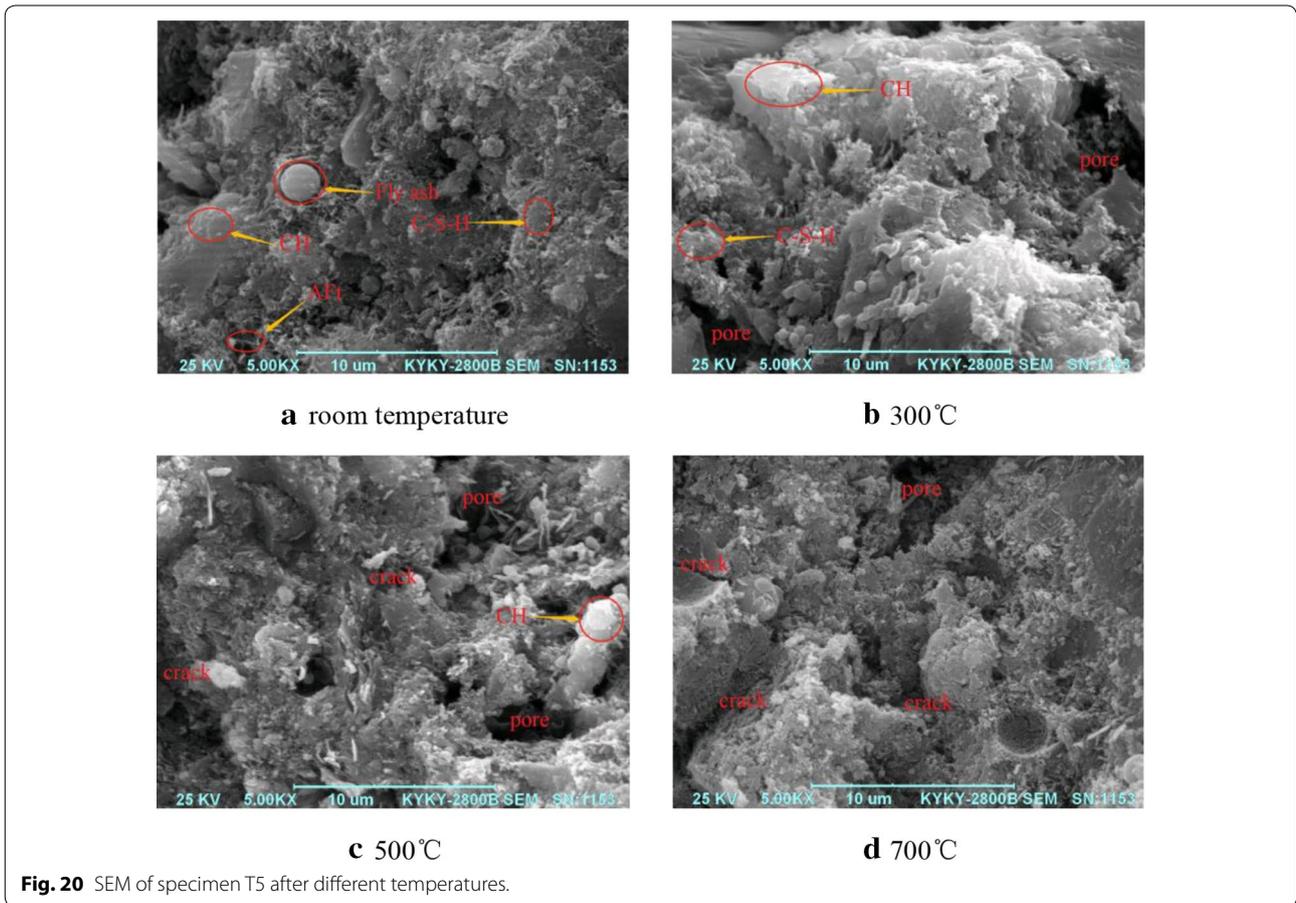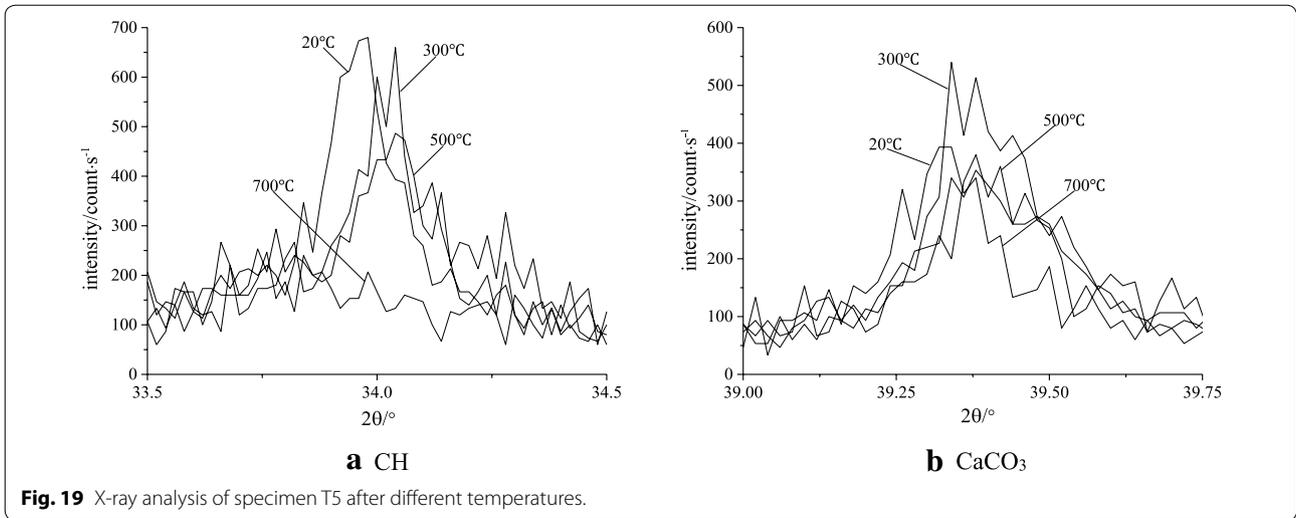
Liu *et al. Int J Concr Struct Mater* (2020) 14:26

Page 13 of 15

Fig. 19 X-ray analysis of specimen T5 after different temperatures.

Fig. 20 SEM of specimen T5 after different temperatures.

influence of temperature on the microstructure of concrete produced with desert sand, the microscopic experiments (XRD, SEM) were employed. Based on the analysis of experimental results, the major conclusions were summarized in the following.

1. The mass loss rate of concrete produced with desert sand increased with temperature under two cooling regimes. The mass loss rate of concrete produced with desert sand under the condition of water cool-

Liu *et al. Int J Concr Struct Mater* (2020) 14:26

Page 14 of 15

ing was less than that under the condition of natural cooling.

2. The elasticity modulus under static compression and prismatic compressive strength of concrete produced with desert sand declined with temperature. Whereas, the cubic compressive strength of concrete produced with desert sand increased firstly, and then declined with temperature. When the temperature amounted to 100 °C, the cubic compressive strength of concrete produced with desert sand reached the maximum value.

3. The elasticity modulus under static compression, cubic compressive strength and prismatic compressive strength of concrete produced with desert sand after elevated temperature increased firstly, and then declined with DSRR. When DSRR was equal to 40%, the elasticity modulus under static compression, cubic compressive strength and prismatic compressive strength of concrete produced with desert sand reached the maximum value.

4. Regression models among the mechanical performances of concrete produced with desert sand, DSRR and temperature were established, the determination coefficients of which were above 0.95. So these models were effective to predict the mechanical behaviors of concrete produced with desert sand after elevated temperature.

5. According to microscopic experiments, concrete produced with desert sand at room temperature was inner structurally-complete and had good compactness. The interface between coarse aggregate and cement mortar became more distinct after 300 °C. After 500 °C, the dimension of intact layered CH decreased. Many small pores were produced. After 700 °C, cement matrix became more shriveled. White large crystals CH were scarce.

Author details
[1] College of Civil and Hydraulic Engineering, Ningxia University, Yinchuan 750021, China. [2] Xinhuan College, Ningxia University, Yinchuan 750021, China. [3] College of Transportation Engineering, Tongji University, Shanghai 201800, China.

References

Al-Harthy, A. S., Abdel Halim, M., & Taha, R. (2007). The properties of concrete made with fine dune sand. *Construction and Building Materials, 21,* 1803–1808.

Ali, B., & Hasan, Z. (2008). Effects of silica fume addition and water to cement ratio on the properties of high-strength concrete after exposure to high temperatures. *Cement & Concrete Composites, 30,* 106–112.

Al-Sanad, H. A., Ismael, N. F., & Nayfeh, A. J. (1993). Geotechnical properties of dune sands in Kuwait. *Engineering Geology, 34,* 45–52.

Canbaz, M. (2014). The effect of high temperature on reactive powder concrete. *Construction and Building Materials, 70,* 508–513.

Chaabane, L. A., Kadri, E. H., & Yahia, S. (2017). Dune sand and pumice impact on mechanical and thermal lightweight concrete properties. *Construction and Building Materials, 133,* 209–218.

Chinese Standard. (2002). *Standard for test method of mechanical properties on ordinary concrete (GB/T 50081-2002)*. Beijing: China Building Industry Press. **(In Chinese)**.

Chuah, S., Duan, W. H., & Pan, Z. (2016). The properties of fly ash based geopolymer mortars made with dune sand. *Materials and Design, 92,* 571–578.

Gao, Y. S., Chen, R. N., & Li, Y. H. (2013). *Engineering utility and properties of desert aeolian sand in China*. Beijing: China Water and Power Press. **(in Chinese)**.

Guo, Z. H., & Shi, X. D. (2003). *Behaviour of reinforced concrete at elevated temperature and calculation*. Beijing: Tsinghua University Press.

Harun, T., & Ahmet, C. (2008). The effect of high temperature on compressive strength and splitting tensile strength of structural lightweight concrete containing fly ash. *Construction and Building Materials, 22,* 2269–2275.

He, Z. J., & Song, Y. P. (2008). Failure mode and constitutive model of plain high-strength high- performance concrete under bi-axial compression after exposure to high temperatures. *Acta Mechanica Solida Sinica, 21,* 149–159.

Hiremath, P. N., & Yaragal, S. C. (2018). Performance evaluation of reactive powder concrete with polypropylene fibers at elevated temperatures. *Construction and Building Materials, 169,* 499–512.

Husem, M. (2006). The effects of high temperature on compressive and flexural strengths of ordinary and high-performance concrete. *Fire Safety Journal, 41,* 155–163.

Isa, Y., Rafat, S., & Ömer, Ö. (2011). Influence of high temperature on the properties of concrete made with industrial by-products as fine aggregate replacement. *Construction and Building Materials, 25,* 967–972.

Ivanka, N., Ivana, K., & Ivica, G. (2011). The effect of high temperatures on the mechanical properties of concrete made with different types of aggregates. *Fire Safety Journal, 46,* 425–430.

Jin, B. H., Song, J. X., & Liu, H. F. (2012). Engineering characteristics of concrete made of desert sand from Maowusu sandy land. *Applied Mechanics and Materials, 174–17,* 604–607.

Kim, G. Y., Kim, Y. S., & Lee, T. G. (2009). Mechanical properties of high-strength concrete subjected to high temperature by stressed test. *Transactions of Nonferrous Metals Society of China, 19,* 128–133.

Li, M. (2005). *The fire damage of high strength concrete and its comprehensive evaluation*. Nanjing: Southeast University.

Li, L., Jia, P., & Dong, J. (2017). Effects of cement dosage and cooling regimes on the compressive strength of concrete after post-fire-curing from 800 °C. *Construction and Building Materials, 142,* 208–220.

Liu, H. F., Ma, H. J., Liu, N., et al. (2017a). Influence of fly ash and desert sand on the carbonation resistance property of concrete. *Bulletin of the Chinese Ceramic Society, 36,* 3823–3828+3847.

Liu *et al. Int J Concr Struct Mater*   *(2020) 14:26*

Page 15 of 15

Liu, H. F., Ma, J. R., & Wang, Y. Y. (2017b). Influence of desert sand on the mechanical properties of concrete subjected to impact loading. *Acta Mechanica Solida Sinica, 30,* 583–595.

Liu, H. F., Wang, Y. Y., & Song, J. X. (2016). Numerical simulation of dynamic mechanical behaviors of desert sand concrete. *Journal of Hydraulic Engineering, 47,* 493–500+508.

Padmakumar, G. P., Srinivas, K., & Uday, K. V. (2012). Characterization of aeolian sands from Indian desert. *Engineering Geology, 139–140,* 38–49.

Sakr, K., & El-Hakim, E. (2005). Effect of high temperature or fire on heavy weight concrete properties. *Cement and Concrete Research, 35,* 590–596.

Sun, W., & Miu, C. W. (2012). *Modern concrete theory and technology*. Beijing: Science Press.

Varona, F. B., Baeza, F. J., & Bru, D. (2018). Influence of high temperature on the mechanical properties of hybrid fibre-reinforced normal and high strength concrete. *Construction and Building Materials, 159,* 73–82.

Wang, Z. J., Li, X. A., & Song, Y. S. (2011). *Research on the engineering utility and geotechnical mechanical properties of desert aeolian sand from Mu Us sandy land*. Beijing: Geological Publishing House. **(in Chinese)**.

Zhai, Y., Deng, Z. C., & Li, N. (2014). Study on compressive mechanical capabilities of concrete after high temperature exposure and thermo-damage constitutive model. *Construction and Building Materials, 68,* 777–782.

Zhang, G. X., Song, J. X., & Yang, J. S. (2006). Performance of mortar and concrete made with a fine aggregate of desert sand. *Building and Environment, 41,* 1478–1481.

Zheng, W. Z., Li, H. Y., & Wang, Y. (2012). Compressive behaviour of hybrid fiber-reinforced reactive powder concrete after high temperature. *Materials and Design, 41,* 403–409.

Zhenghu, D., Honglang, X., & Zhibao, D. (2007). Morphological, physical and chemical properties of aeolian sandy soils in northern China. *Journal of Arid Environments, 68,* 66–76.

Publisher's Note